Hindawi
Journal of Spectroscopy
Volume 2017, Article ID 3595078, 9 pages
https://doi.org/10.1155/2017/3595078

Research Article

Longitudinal Raman Spectroscopic Observation of Skin Biochemical Changes due to Chemotherapeutic Treatment for Breast Cancer in Small Animal Model

Myeongsu Seong,[1] NoSoung Myoung,[2] Songhyun Lee,[1] Hyeryun Jeong,[1] Sang-Youp Yim,[2] and Jae Gwan Kim[1,3]

[1]*Department of Biomedical Science and Engineering, Institute of Integrated Technology, Gwangju Institute of Science and Technology, 123 Cheomdan Gwagiro, Bukgu, Gwangju 61005, Republic of Korea*
[2]*Advanced Photonics Research Institute, Gwangju Institute of Science and Technology, 123 Cheomdan Gwagiro, Bukgu, Gwangju 61005, Republic of Korea*
[3]*School of Electrical Engineering and Computer Science, Gwangju Institute of Science and Technology, 123 Cheomdan Gwagiro, Bukgu, Gwangju 61005, Republic of Korea*

Correspondence should be addressed to Sang-Youp Yim; syim@gist.ac.kr and Jae Gwan Kim; jaekim@gist.ac.kr

Received 11 February 2017; Revised 17 May 2017; Accepted 23 May 2017; Published 16 July 2017

Academic Editor: Yusuke Oshima

The cancer field effect (CFE) has been highlighted as one of indirect indications for tissue variations that are insensitive to conventional diagnostic techniques. In this research, we had a hypothesis that chemotherapy for breast cancer would affect skin biochemical compositions that would be reflected by Raman spectral changes. We used a fiber-optic probe-based Raman spectroscopy to perform preliminary animal experiments to validate the hypothesis. Firstly, we verified the probing depth of the fiber-optic probe (~800 μm) using a simple intravenous fat emulsion-filled phantom having a silicon wafer at the bottom inside a cuvette. Then, we obtained Raman spectra during breast cancer treatment by chemotherapy from a small animal model in longitudinal manner. Our results showed that the treatment causes variations of biochemical compositions in the skin. For further validation, the Raman spectra will have to be collected from more populations and spectra will need to be compared with immunohistochemistry of the breast tissue.

1. Introduction

Cancer field effect (CFE) has been highlighted since it could unveil minute chemical changes in the region of interest that cannot be captured by clinical or histological diagnostic techniques. Since first finding of CFE from oral cancers in 1953 [1], studies related to CFE have been gradually increased [2, 3]. While other techniques including microscopy, polymerase chain reaction (PCR), and immunohistochemistry were utilized to study CFE [3–6], Raman spectroscopy has been spotlighted as a useful tool since it has been shown that the spectroscopy can detect changes that are insensitive to histological evaluation implying that chemical changes are not local and proceed earlier than anatomical or physical changes [7–9]. Such studies proved the ability of Raman spectroscopy as a dominant candidate for a sensitive and minimally invasive optical biopsy tool. Based on the results from the previous studies, we hypothesized that breast cancer treatment may induce biochemical changes in the skin because they are adjacent to each other. The objective of this study was to find the possibility utilizing skin biochemical alternations to monitor breast cancer treatment. To our best of knowledge, there has been no report about skin biochemical alternation due to breast cancer treatment to date. In this paper, we show that the probe has limited maximum probing depth of about 800 μm (shallower than the thickness of the skin of a rat, 1.5 mm~ [10]) and longitudinal biochemical changes by breast cancer treatment in a small animal model ($n = 4$).

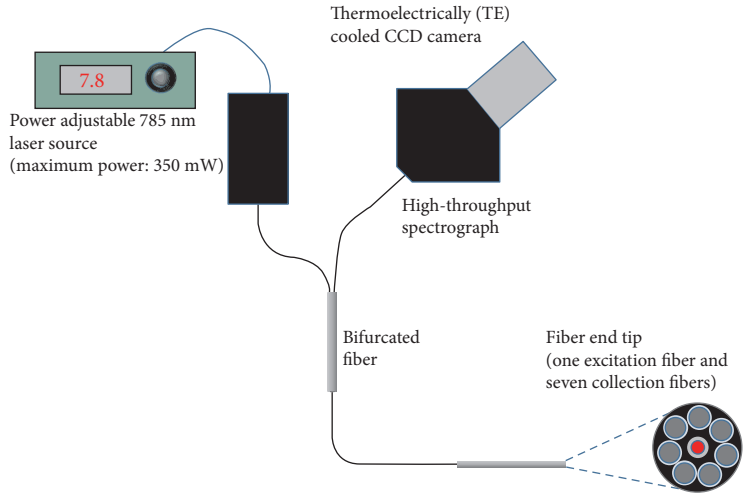

Figure 1: Schematic of the Raman system. One centered excitation fiber and seven surrounding collection fibers were configured as a bifurcated fiber. A power adjustable 785 nm laser source (maximum power: 350 mW) coupled with the excitation fiber was used as the excitation source, and a thermoelectrically (TE) cooled CCD camera coupled to a high-throughput spectrograph collects spontaneous Raman signals transmitted through the seven collection fibers.

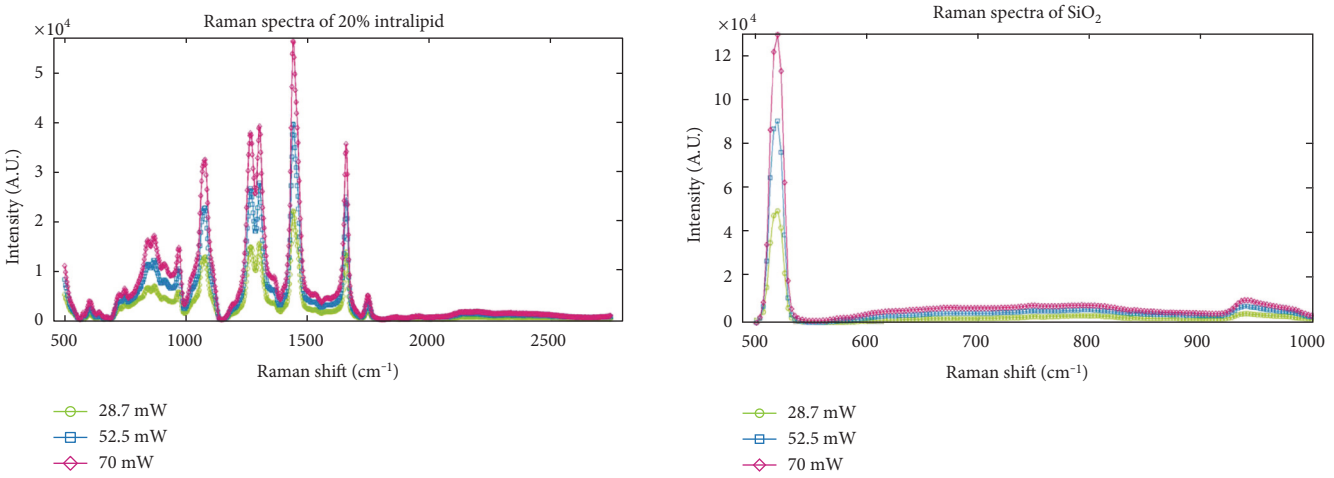

Figure 2: (a) Spectra of 20% intralipid solution after autofluorescence suppression and (b) spectra of a silicon wafer (SiO_2) measured with laser optical powers of 28.7 mW (empty diamond, magenta), 52.5 mW (empty square, blue), and 70 mW (empty circle, green). No peak shift or spectral change was observed from power adjustment.

2. Materials and Methods

2.1. Configuration and Calibration of a Fiber-Optic Raman System. Figure 1 shows the schematic of a fiber-optic Raman system used in the study. The Raman system has a power adjustable 785 nm laser diode (FC-785-350-MM2-PC-1-0-RM, 350 mW of maximum power, RGBLase) as a laser source, a high-throughput spectrograph (XPE85-NIR, F/1.4, Nanobase) coupled with a thermoelectrically (TE) cooled charge coupled device (CCD) camera (iDus 401 BR-DD, Andor) for light collection and data transfer. A fiber-optic probe (Emvision *LLC*) with one centered excitation fiber (200 μm core) and seven surrounding collection fibers (300 μm core) and a plano-convex lens that covers in front of the fibers limiting the working distance of the probe to be 0–400 μm specified in the specification sheet. The excitation fiber is coupled to the laser source, and seven surrounding collection fibers are coupled with a spectrograph for back-scattered spontaneous Raman signal delivery. In order to assure transmission of the wavelength of 785 nm through excitation path and the wavelengths longer than 785 nm through collection path, a band pass filter and a long pass filter were placed in the paths, respectively. Raman shifts measured range approximately from 500 cm^{-1} to 2800 cm^{-1}. The spectral resolution of the device was 11 cm^{-1}.

2.2. Probing Depth Validation Using a Simple Liquid Phantom. In order to make sure its probing depth is limited

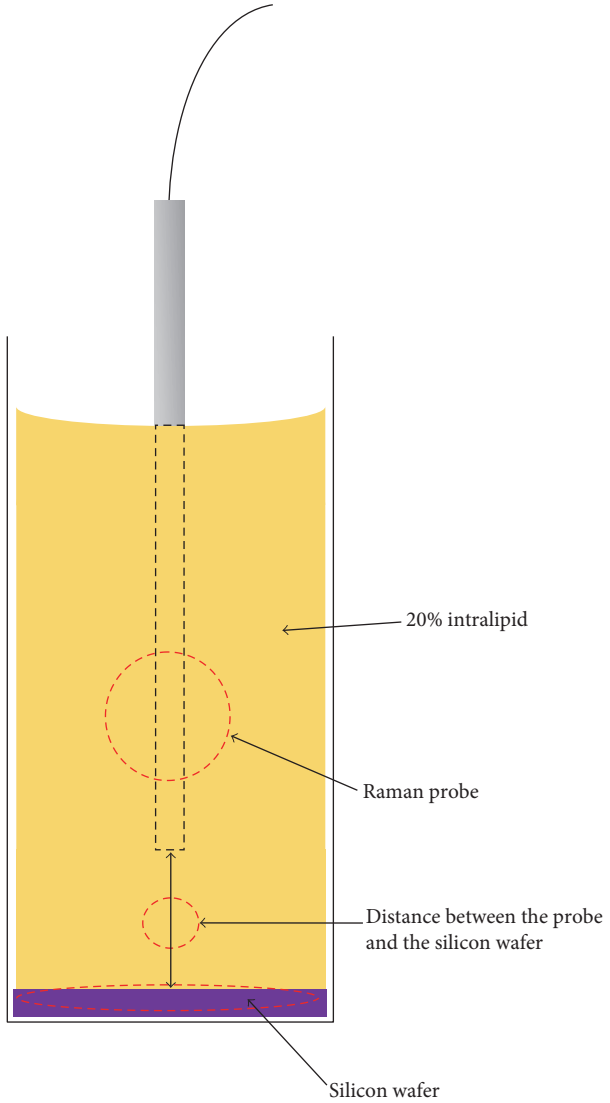

Figure 3: Schematic of a setup to check the sensitive depth of the Raman probe. A silicon wafer was placed at the bottom in a cuvette. The cuvette was filled with 20% intralipid solution. Raman probe was immersed in the intralipid solution. The distance between the silicon wafer and the probe end tip was varied from 0 μm to 1000 μm incrementing the distance by 100 μm using a one-axis linear translation stage.

to the specific depth, we made a simple intravenous fat emulsion-filled liquid (intralipid 20%, Fresenius Kabi) phantom having a silicon oxide wafer as the bottom. The intralipid was utilized since that has been used in previous Raman researches as a human tissue mimetic phantom [11]. Also, the silicon wafer was used because intralipid has no characteristic peak nearby 520 cm^{-1} while the silicon wafer has strong characteristic peak nearby 520 cm^{-1}. Spectra of 20% intralipid and a silicon wafer were acquired with different optical power of the source (28.7 mW, 52.5 mW, and 70 mW) as the references. Figure 2 shows the measured spectra of 20% intralipid (Figure 2(a)) and silicon wafer (Figure 2(b)). Figure 3 shows a schematic of measurement setup for probing depth validation. For determining the working distance of the Raman

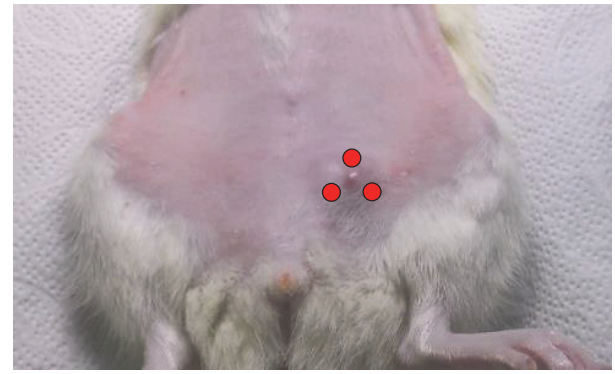

Figure 4: An example of shaved and depilated animal. Among eight nipples, one abdominal nipple with breast tumor was monitored in the study. Raman signals were measured in triangular shape around a tumor (red colored dots). Below the right nipple, breast cancer cells (~1 million) were inoculated into mammary fat pad subcutaneously.

probe, Raman spectra were collected varying distances between the silicon wafer and the probe from 0 μm (fully contact) to 1000 μm with a step of 100 μm distance increment. The laser power was set to 28.7 mW for the validation. The distance was carefully varied by using a one-axis linear translation stage (MT01, Thorlabs).

2.3. Animal Model. Fischer 344 female rats (160 g–220 g, Japan SLC) were used in the study. After baseline measurement, about one million 13762 MAT B-III breast cancer cells (CRL-1666, ATCC) were inoculated to lateral caudal abdominal breast (right nipple on Figure 4) of each rat to induce breast tumor growth. When the tumor size became 8 mm, single high dose (100 mg/kg) of cyclophosphamide (C0768-5G, Sigma Aldrich) solution, an alkylating agent that interferes cancer cell growth by preventing deoxyribonucleic acid (DNA) replication and ribonucleic acid (RNA) creation, was intraperitoneally injected as chemotherapy treatment. During the experimental period, the tumor size was measured by a caliper. The breast cancer animal model was chosen since the model is a well-established animal model in breast cancer study (13762 MAT B-III breast cancer cell line is highly tumorigenic in Fischer 344 since the cell line is derived from the strain of Fischer 344 itself) [12–14]. Cyclophosphamide was used because the chemical has been used as a chemotherapeutic agent for treating human [15–17] and rat [14, 18] breast tumors in previous researches. All the animal experiments were approved by the Gwangju Institute of Science and Technology Institutional Review Board.

2.4. Longitudinal Animal Measurements. For all the animals, fur on the belly was shaved and depilated to reduce scattering due to fur. Figure 4 shows an example of a shaved and then depilated belly of an animal. During measurement, each animal was under general anesthesia by 1% to 2% of isoflurane mixed with breathing gas (21% O_2 and 79% N_2). In case of animals with breast tumor, Raman spectra from three sites around the tumor were acquired in each measurement. In case of animals without the tumor, the Raman spectra were

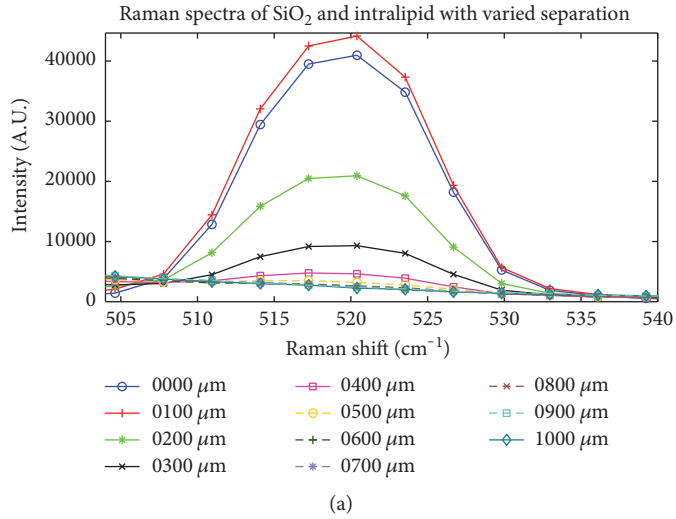

(a)

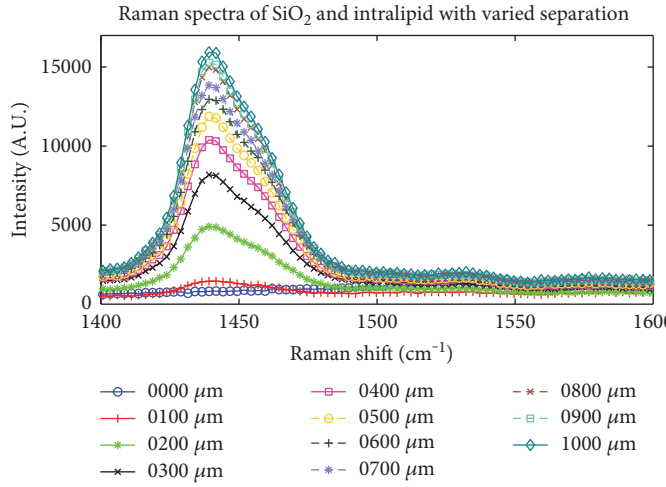

(b)

Figure 5: Decay of silicon wafer's characteristic peak and increase of intralipid's one characteristic peak while the distance between the silicon wafer and the probe end tip increases in the phantom measurement as shown in Figure 3. The laser power was fixed to 28.7 mW. Notice that from full contact to 100 μm separation, the Raman characteristic peak of the silicon increases and it might happen in the combination of the mismatch of refractive indices between intralipid, silicon wafer, and the probe and the effect of the plano-convex lens in front of the excitation and detection fibers. Mixture of characteristic peaks of the silicon and intralipid still exists till the distance of 800 μm, and it implies that when measuring highly scattering medium in near-infrared (NIR) range such as the biological tissues, the working distance of the probe would be longer than the one described in the specification.

acquired around the nipple three times with triangular shape. Multiple measurements were done to minimize the effect of heterogeneity of the tissue. Figure 4 also shows an example of Raman signal acquisition points. The total integration time for one Raman signal measurement was 10 seconds (100 times summation of Raman signal acquired in 0.1 second). Animals were grouped into three groups: rat group ($n = 4$), no chemo group ($n = 3$), and chemo only group ($n = 2$). Breast tumor growth was induced for both rat group and no chemo group by inoculating about one million breast cancer cells to the mammary fat pad. The tumor was treated by cyclophosphamide injection when tumor size reached to about 8 mm for rats in rat group and the Raman measurement was started. For no chemo group, the Raman spectra were acquired when tumor size became about 8 mm and no chemotherapy was performed. Chemo only group did not have breast cancer cell inoculation while cyclophosphamide was administered to observe effects of

Table 1: The tumor volume variation from the four rats in the rat group.

	Rat 1 (tumor volume, mm^3)	Rat 2 (tumor volume, mm^3)	Rat 3 (tumor volume, mm^3)	Rat 4 (tumor volume, mm^3)
Baseline	432.63	172.76	656.57	467.24
Day 1	603.85	615.19	1017.24	631.27
Day 2	1065.68	569.64	1350.13	789.19
Day 3	781.20	434.11	865.37	862.11
Day 4	539.50	390.18	864.33	606.29

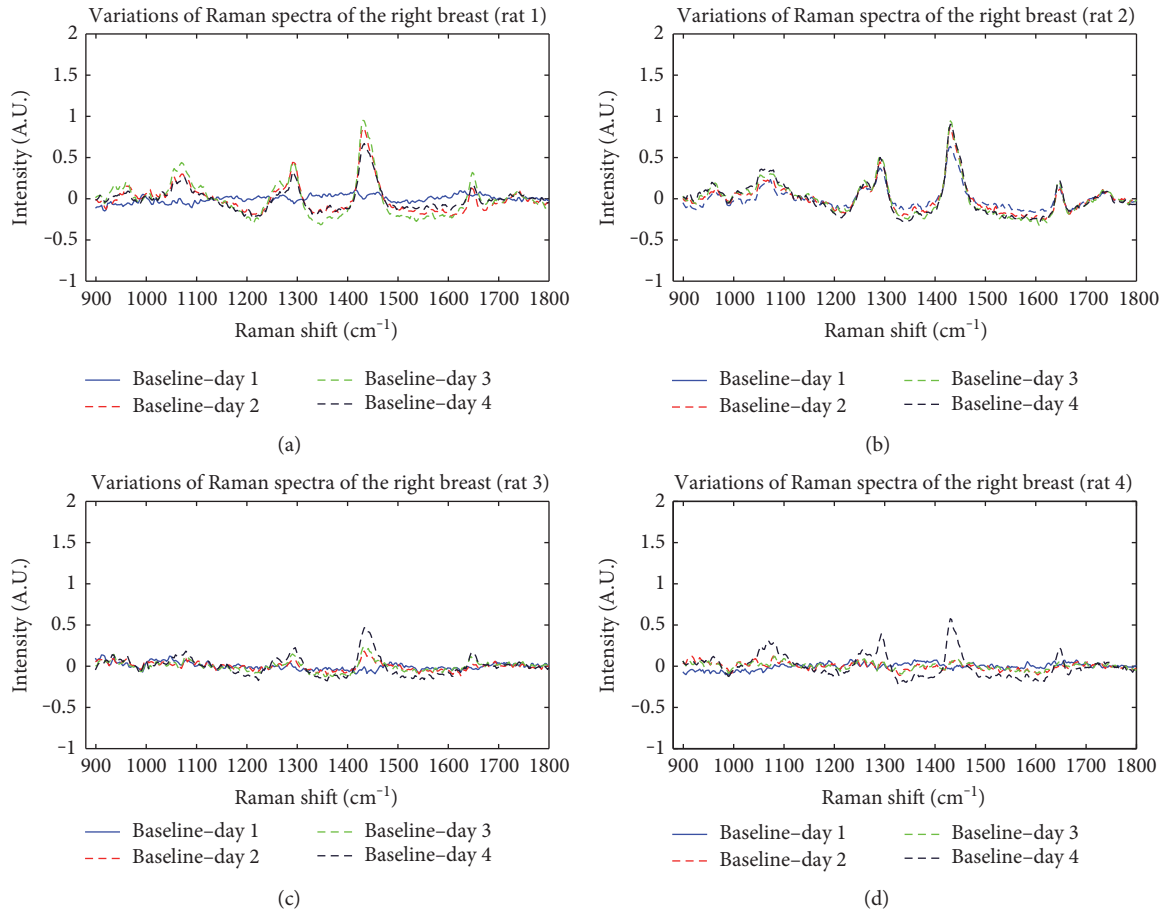

Figure 6: Variations of Raman spectra from rat group with regard to the baseline (baseline means the day high-dose chemotherapy was started). The spectrum for each day was subtracted from the baseline signal. Positive values mean that the intensity was decreased, and the negative values mean that the intensity was increased with respect to the baseline signal. Day n means n day postchemotherapy.

only cyclophosphamide on skin chemical compositions. The laser power was adjusted lower than 28 mW not to damage the tissue. In case of tumor-bearing rats, the tumor volume was calculated by an equation of ellipsoid volume.

2.5. Preprocessing and Data Analysis. Raw bio-Raman signals are mostly mixed signals of autofluorescence and pure Raman signals when 785 nm of excitation beam is used. Since the autofluorescence obscures Raman spectrum, all the spectra were fitted using modified polyfit method, and the fitted autofluorescence was subtracted following fluorescence subtraction procedure by Lieber and Mahadevan-Jansen [19] except Raman spectra of silicon wafer. Also, all the animal Raman spectra were smoothed by a Savitzky-Golay filter (third order, window size: 5). The smoothed Raman spectra were mean centered by subtracting one's mean intensity from each spectrum's intensity and normalized with respect to the mean intensity. All the preprocessing scripts were written and performed using Mathematica 9.0 (Wolfram) and MATLAB R2013b (Mathworks). The spectral range from 900 cm^{-1} to 1800 cm^{-1} was used since the range has rich chemical information of lipid, protein, and more [20]. Note that no chemometric technique was used in the study due to limited number of samples and objective of the study (longitudinal observation of biochemical composition changes).

Table 2: The tumor volume variation from the three rats in the no chemo group.

	No chemo 1 (tumor volume, mm^3)	No chemo 2 (tumor volume, mm^3)	No chemo 3 (tumor volume, mm^3)
Baseline	58.99	22.86	51.62
Day 1	125.34	48.49	107.23
Day 2	216.03	105.32	169.59
Day 6	2161.48	1096.82	2509.94

3. Results and Discussion

3.1. Probing Depth Validation Using a Simple Liquid Phantom. The characteristic peaks of intralipid and silicon wafer are shown in Figure 2(a) and Figure 2(b), respectively. Source power changes did not cause any effect on the characteristic peaks except intensity increments. Figure 5 shows the characteristic peaks of silicon wafer (Figure 5(a)) and intralipid (Figure 5(b)) gradually decrease and increase as the distance between the silicon wafer and the probe end becomes longer, respectively. When the distance reached 800 μm, the

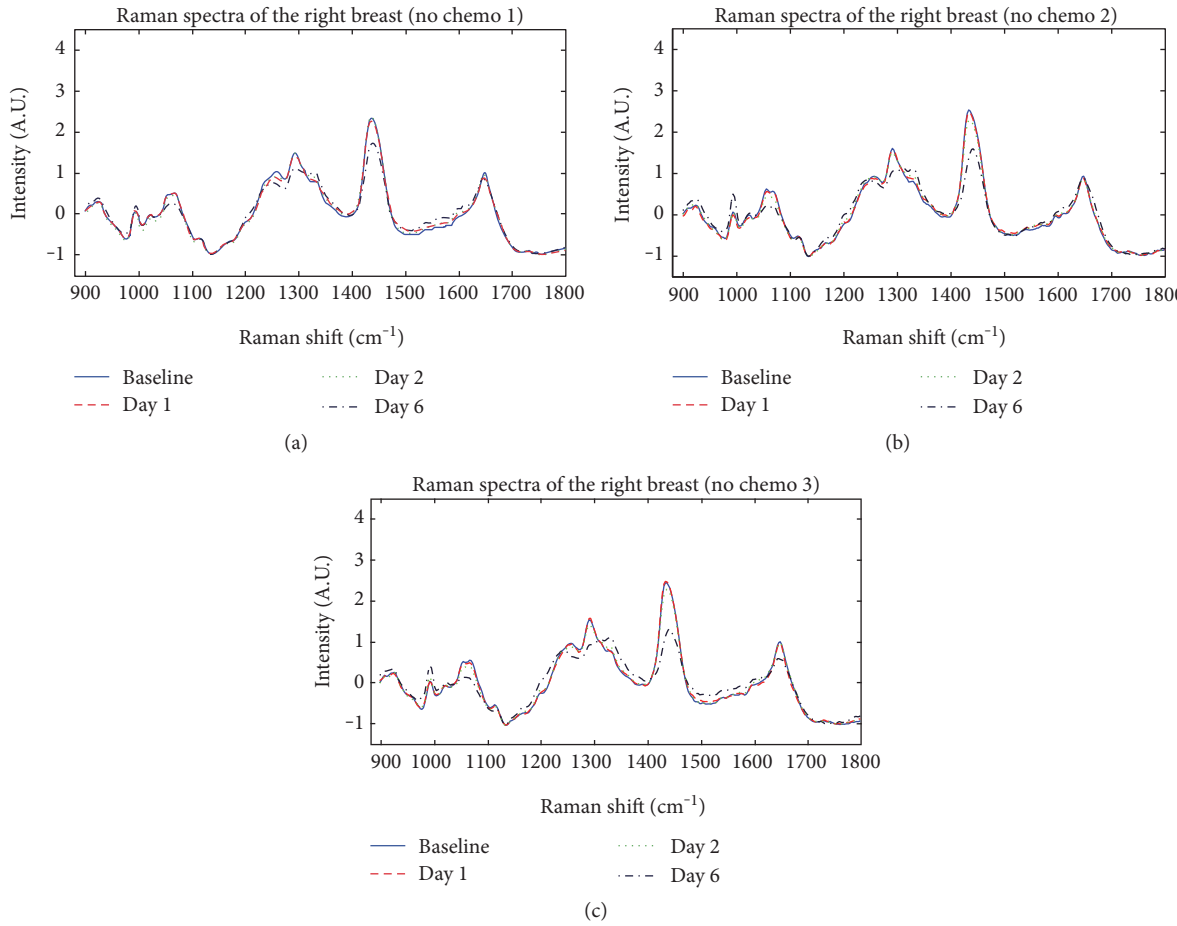

Figure 7: Variation of Raman spectra with breast tumor growth and without breast cancer treatment (no chemo group, baseline means the day high-dose chemotherapy was started). Day n means n day postchemotherapy.

characteristic peaks of the silicon wafer and intralipid reached their extrema showing no changes with longer separations. The result shows that the probing depth of the Raman probe used in this study is mostly limited to 0–800 μm. The range of the working distance was longer than the values in the specification (0–400 μm). This may come from scattering dominant nature of phantom [21–23]. We also notice that while the separation varies from 0 μm to 100 μm, the Raman characteristic peak of the silicon increases and it might happen in the combination of the mismatch of refractive indices between intralipid, silicon wafer, and the probe and the effect of the plano-convex lens in front of the excitation and detection fibers.

3.2. Longitudinal Animal Measurements

3.2.1. Rat Group. Table 1 and Figure 6 show the tumor volume changes and relative variations of Raman spectra from the baseline, respectively. The Raman spectra before subtraction are not shown here because the variation was minute. Baseline means day 0 from the chemotherapy. In other words, the chemotherapeutic agent was injected on the day 0. Tumor size for rat 2 regressed earliest and the Raman spectrum was immediately changed on day 1 (Figure 6(b)). Rat 3 had the biggest tumor size when chemotherapy was started, and the Raman spectra showed minute change as the days passed (Figure 6(c)). Also, the Raman spectrum on day 1 did not show distinct change with respect to the baseline signal. Rat 4 showed delayed response regressing the tumor size from the day 4. The Raman spectra variation was matched as the tumor regression day showing the clear change of Raman spectrum on day 4 while there was no significant Raman spectral variation from day 1 to day 3. Among rat 1 to rat 4, rat 1 showed moderate response that the tumor regressed from day 3. The significant variation was happening around 1064 cm^{-1} (lipid), 1265–1267 cm^{-1} (collagen, protein, and lipid), 1299–1303 cm^{-1} (lipid, fatty acids, collagen, and protein), 1440 cm^{-1} (lipid), 1445 cm^{-1} (protein), and 1654–1656 cm^{-1} (protein and lipid) [20, 24]. The peaks or Raman shifts are known as the positions related to lipid and protein components [20]. It reflects that tumor regression due to chemotherapeutic agent causes variations of lipid and protein components in the skin because the probing depth for the probe is limited to the depth of skin as shown in the Section 3.1.

3.2.2. No Chemo Group. Table 2 and Figure 7 show the tumor volume changes and the Raman spectra on the measurement days, respectively. While day 1 and day 2 Raman spectra did not show any significant variation with respect to the baseline

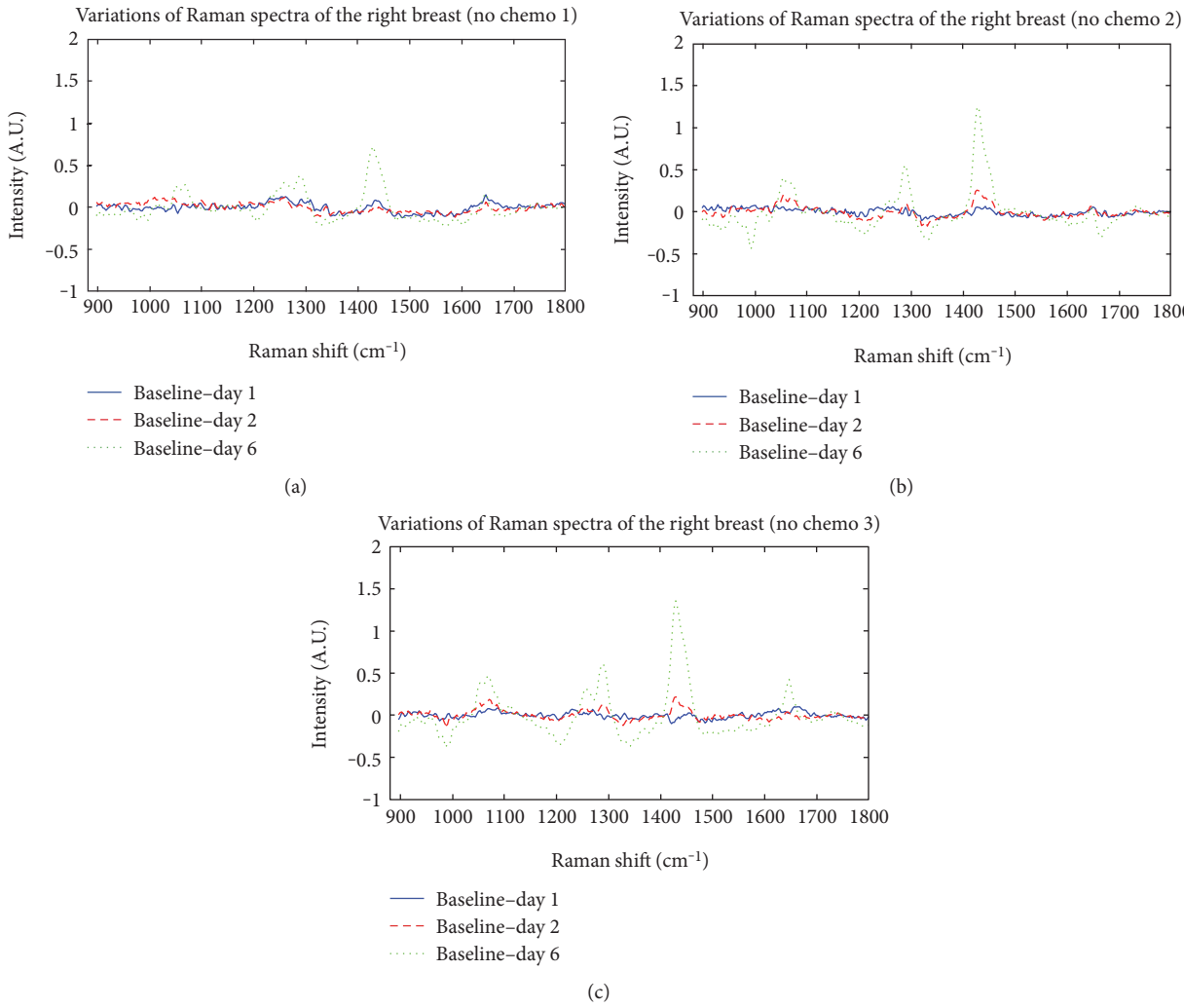

Figure 8: Variations of Raman spectra with regard to the baseline (no chemo group). The spectrum for each day was subtracted from the baseline signal. Positive values mean that the intensity was decreased, and the negative values mean that the intensity was increased with respect to the baseline signal. Day n means n day postchemotherapy.

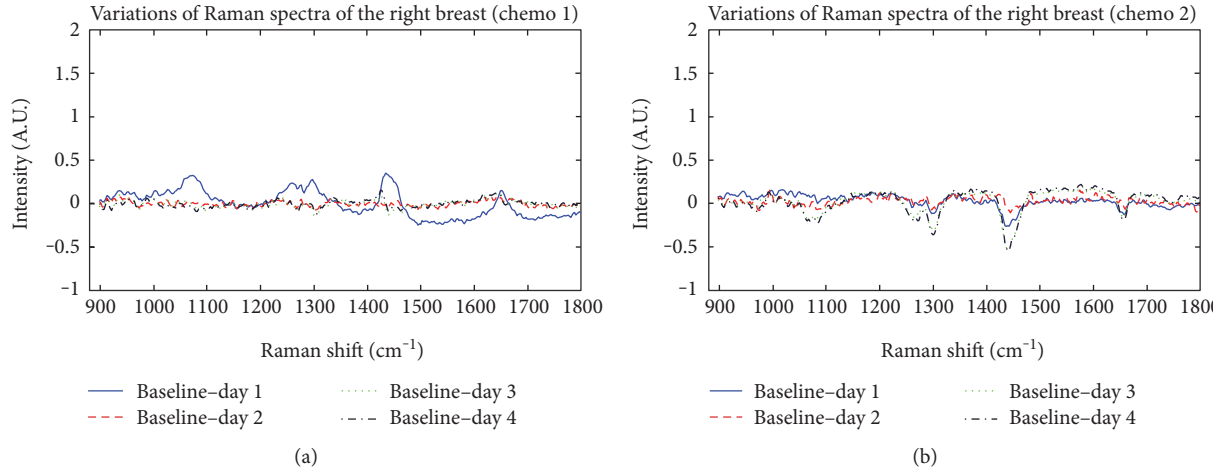

Figure 9: Variations of Raman spectra with regard to the baseline (chemo only group, baseline means the day high-dose chemotherapy was started). No breast tumor growth was induced. Day n means n day postchemotherapy.

signal, Raman spectra on day 6 from the baseline show degradation of peaks around 1299–1303 cm^{-1} and the peak height around 1440 cm^{-1} and 1445 cm^{-1}. When tumor size reached to similar size as the one in the rat group, the Raman spectra vary in a different way from the spectra in the rat group showing the possibility of monitoring breast cancer treatment from the external tissue. Because there were studies showing tissue composition changes either 1 cm or 7 cm away from the tumor region [3, 5], Raman spectral variations on the skin due to breast cancer treatment and breast cancer growth without treatment are also possible. Figure 8 shows the variations of Raman spectra from the baseline. Comparing Figure 6 and Figure 8, significant difference in Raman spectral region of 1000–1003 cm^{-1} (protein) [24] between the rat group and no chemo group can be found.

3.2.3. Chemo Only Group. Figure 9 shows variations of Raman spectra from day 0 (chemotherapeutic agent injection) for two rats. The Raman spectral variations were distinct from the changes in the rat group and no chemo group. Our data show that administration of cyclophosphamide causes the peak variations in 1090–1100 cm^{-1} (lipid/phospholipid DNA backbone), 1280–1282 cm^{-1} (collagen), and 1447–1450 cm^{-1} (DNA/RNA protein lipid) [24]. There were previous researches showing that high dose of cyclophosphamide affects the skin especially for protein/collagen components [25, 26], and our data correlate well with the previous studies.

Meanwhile, chemo only group did not show any variation in 1200 cm^{-1} while rat group shows the peak variation nearby 1200 cm^{-1} (protein) [24]. In addition, the two rats showed different response from the same chemotherapeutic agent injection. This discrepancy might come from the physiological differences between the rats. The different response is another subject that needs further investigation to seek any possibility as the early prediction factor of chemotherapeutic efficacy for a specific chemotherapeutic agent.

4. Conclusion

Here, we had hypothesized that breast tumor treatment would influence neighboring tissue (here skin) varying chemical compositions of the tissue and showed the skin Raman spectral changes while breast cancer was treated. The study suggests the possibility of monitoring tumor treatment located relatively deep such as breast cancer. From our results, we could distinguish the three groups from the peak variations in the Raman shifts of 1000–1003 cm^{-1}, 1125–1132 cm^{-1}, and 1200 cm^{-1}. To the authors' best of knowledge, there was no study about variations of chemical compositions in neighboring tissue due to breast cancer treatment; this preliminary result will require additional validations such as comparison of the Raman spectra with immunohistochemistry.

Conflicts of Interest

The authors declare that there is no conflict of interests regarding the publication of this article.

Authors' Contributions

Myeongsu Seong and NoSoung Myoung contributed equally to this work.

Acknowledgments

This work is supported by the Research on Advanced Optical Science and Technology grant (Sang-Youp Yim) funded by the Gwangju Institute of Science and Technology (GIST) and "Biomedical Integrated Technology Research" Project through a grant (Jae Gwan Kim) provided by GIST in 2017, the National Research Foundation of Korea Grant 2012K1A2B1A03000757 (Jae Gwan Kim), and Basic Science Research Program through the NRF funded by the Ministry of Education, Science and Technology 2013R1A1A2013625 (Jae Gwan Kim) and 2013R1A1A2058746 (NoSoung Myoung).

References

[1] D. P. Slaughter, H. W. Southwick, and W. Smejkal, "Field cancerization in oral stratified squamous epithelium. Clinical implications of multicentric origin," *Cancer*, vol. 6, no. 5, pp. 963–968, 1953.

[2] Z. J. Smith, T. R. Huser, and S. Wachsmann-Hogiu, "Raman scattering in pathology," *Analytical Cellular Pathology*, vol. 35, no. 3, pp. 145–163, 2012.

[3] H. Chai and R. E. Brown, "Review: field effect in cancer-an update," *Annals of Clinical and Laboratory Science*, vol. 39, no. 4, pp. 331–338, 2009.

[4] R. K. Bista, P. Wang, R. Bhargava et al., "Nuclear nanomorphology markers of histologically normal cells detect the 'field effect' of breast cancer," *Breast Cancer Research and Treatment*, vol. 135, no. 1, pp. 115–124, 2012.

[5] C. M. Heaphy, M. Bisoffi, C. A. Fordyce et al., "Telomere DNA content and allelic imbalance demonstrate field cancerization in histologically normal tissue adjacent to breast tumors," *International Journal of Cancer*, vol. 119, no. 1, pp. 108–116, 2006.

[6] M. C. Risk, B. S. Knudsen, I. Coleman et al., "Differential gene expression in benign prostate epithelium of men with and without prostate cancer: evidence for a prostate cancer field effect," *Clinical Cancer Research*, vol. 16, no. 22, pp. 5414–5423, 2010.

[7] E. Vargis, E. M. Kanter, S. K. Majumder et al., "Effect of normal variations on disease classification of Raman spectra from cervical tissue," *Analyst*, vol. 136, pp. 2981–2987, 2011.

[8] M. D. Keller, E. M. Kanter, C. A. Lieber et al., "Detecting temporal and spatial effects of epithelial cancers with Raman spectroscopy," *Disease Markers*, vol. 25, no. 6, pp. 323–337, 2008.

[9] S. P. Singh, A. Sahu, A. Deshmukh, P. Chaturvedi, and C. M. Krishna, "In vivo Raman spectroscopy of oral buccal mucosa: a study on malignancy associated changes (MAC)/cancer field effects (CFE)," *Analyst*, vol. 138, pp. 4175–4182, 2013.

[10] B. Wagner, C. Tan, J. L. Barnes et al., "Nephrogenic systemic fibrosis: evidence for oxidative stress and bone marrow-derived fibrocytes in skin, liver, and heart lesions using a 5/6 nephrectomy rodent model," *The American Journal of Pathology*, vol. 181, no. 6, pp. 1941–1952, 2012.

[11] M. Agenant, M. Grimbergen, R. Draga, E. Marple, R. Bosch, and C. van Swol, "Clinical superficial Raman probe aimed for epithelial tumor detection: phantom model results," *Biomedical Optics Express*, vol. 5, no. 4, pp. 1203–1216, 2014.

[12] A. K. Laust, B. W. Sur, K. Wang, B. Hubby, J. F. Smith, and E. L. Nelson, "VRP immunotherapy targeting neu: treatment efficacy and evidence for immunoediting in a stringent rat mammary tumor model," *Breast Cancer Research and Treatment*, vol. 106, no. 3, pp. 371–382, 2007.

[13] T. P. Archer, P. Bretscher, and B. Ziola, "Immunotherapy of the rat 13762SC mammary adenocarcinoma by vaccinia virus augmentation of tumor immunity," *Clinical & Experimental Metastasis*, vol. 8, no. 6, pp. 519–532, 1990.

[14] V. K. Todorova, Y. Kaufmann, and V. S. Klimberg, "Increased efficacy and reduced cardiotoxicity of metronomic treatment with cyclophosphamide in rat breast cancer," *Anticancer Research*, vol. 31, no. 1, pp. 215–220, 2011.

[15] A. Howell, W. D. George, D. Crowther et al., "Controlled trial of adjuvant chemotherapy with cyclophosphamide, methotrexate, and fluorouracil for breast cancer," *Lancet*, vol. 324, no. 8398, pp. 307–311, 1984.

[16] C. Zhou, R. Choe, N. Shah et al., "Diffuse optical monitoring of blood flow and oxygenation in human breast cancer during early stages of neoadjuvant chemotherapy," *Journal of Biomedical Optics*, vol. 12, no. 5, article 51903, 2013.

[17] M. Ayers, W. F. Symmans, J. Stec et al., "Gene expression profiles predict complete pathologic response to neoadjuvant paclitaxel and fluorouracil, doxorubicin, and cyclophosphamide chemotherapy in breast cancer," *Journal of Clinical Oncology*, vol. 22, no. 12, pp. 2284–2293, 2004.

[18] J. P. Sleeman, U. Kim, J. LePendu et al., "Inhibition of MT-450 rat mammary tumour growth by antibodies recognising subtypes of blood group antigen B," *Oncogene*, vol. 18, no. 31, pp. 4485–4494, 1999.

[19] C. A. Lieber and A. Mahadevan-Jansen, "Automated method for subtraction of fluorescence from biological Raman spectra," *Applied Spectroscopy*, vol. 57, no. 11, pp. 1363–1367, 2003.

[20] L. Raniero, R. A. Canevari, L. N. Z. Ramalho et al., "In and ex vivo breast disease study by Raman spectroscopy," *Theoretical Chemistry Accounts*, vol. 130, no. 4–6, pp. 1239–1247, 2011.

[21] S. Jacques, "Optical properties of intralipid," January 2017, http://omlc.org/spectra/intralipid/.

[22] S. T. Flock, S. L. Jacques, B. C. Wilson, W. M. Star, and M. J. C. van Gemert, "Optical properties of intralipid: a phantom medium for light propagation studies," *Lasers in Surgery and Medicine*, vol. 12, no. 5, pp. 510–519, 1992.

[23] H. J. van Staveren, C. J. M. Moes, J. van Marie, S. A. Prahl, and M. J. C. van Gemert, "Light scattering in intralipid-10% in the wavelength range of 400–1100 nm," *Applied Optics*, vol. 30, no. 31, p. 4507, 1991.

[24] R. E. Kast, S. C. Tucker, K. Killian, M. Trexler, K. V. Honn, and G. W. Auner, "Emerging technology: applications of Raman spectroscopy for prostate cancer," *Cancer Metastasis Reviews*, vol. 33, no. 2-3, pp. 673–693, 2014.

[25] H. Wie, L. B. Engesaeter, and E. I. Beck, "Effects of cyclophosphamide on mechanical properties of bone and skin in rats," *Acta Orthopaedica Scandinavica*, vol. 50, pp. 629–634, 1979.

[26] H. Wie and E. I. Beck, "Synthesis and solubility of collagen in rats during recovery after high-dose cyclophosphamide administration," *Acta pharmacologica et toxicologica*, vol. 48, no. 4, pp. 294–299, 2009.